Silver or Gold? A comparison of nanoparticle modified electrochemical genosensors based on cobalt porphyrin-DNA

Kamila Malecka,[a,‡] *Balwinder Kaur,*[a,‡] *D. Andrea Cristaldi,*[b,‡] *Clarissa S. Chay,*[b,‡] *Iwona Mames,*[b,‡] *Hanna Radecka,*[a] *Jerzy Radecki*[a,*], *Eugen Stulz*[b,*]

[a] Institute of Animal Reproduction and Food Research, Polish Academy of Sciences, Tuwima 10, 10-748 Olsztyn, Poland.

[b] School of Chemistry and Institute for Life Sciences, University of Southampton, Highfield, Southampton SO17 1BJ, UK.

‡ *These authors contributed equally to the work*

[*]Corresponding authors: *E-mail: est@soton.ac.uk, j.radecki@pan.olsztyn.pl;*

Abstract

We applied a cobalt-porphyrin modified DNA as electrochemical marker, which was attached to nanoparticles, to detect specific DNA sequences. We compare the performance of gold and silver NPs in oligonucleotide sensors to determine if a change in metal will lead to either higher sensitivity or different selectivity, based on the redox behaviour of silver *vs.* gold. Surprisingly, we find that using either gold or silver NPs yields very similar overall performance. The electrochemical measurements of both types of sensors show the same redox behaviour which is dominated by the cobalt porphyrin, indicating that the electron pathway does not include the NP, but there is direct electron transfer between the porphyrin and the electrode. Both sensors show a linear response in the range of 5×10^{-17} – 1×10^{-16} M; the limit of detection (LOD) is 3.8×10^{-18} M for the AuNP sensor, and 5.0×10^{-18} M for the AgNP sensor, respectively, which corresponds to the detection of about 20 to 50 DNA molecules in the analyte. Overall, the silver system results in a better DNA economy and using cheaper starting materials for the NPs, thus shows better cost-effectivness and could be more suitable for the mass-production of highly sensitive DNA sensors.

Keywords: Silver nanoparticles, gold nanoparticles, Cobalt porphyrin, Electrochemical genosensor, Ultrasensitive detection

1. Introduction

Considering that time and precision is always of essence in diagnostics, there is a continuous search for improved analytical methods which are more sensitive, selective, cost effective and easy to handle [1-5]. The current COVID-19 situation has clearly demonstrated this need on a global scale. The use of electrochemical biosensors, which have been designed to detect known markers such as proteins, nucleic acids and antigens, is very attractive to rapidly diagnose diseases, including viruses. The electrochemical sensors offer advantages such as high sensitivity, operational simplicity, short response times, cost effectiveness and portability, allowing for point-of-care diagnostics as well as usage in the field. Different mechanisms for signal generation are used, including direct oxidation or reduction of nucleic acids [6], modification of the electrode with active layers which are stimulated by free diffusion of redox markers [7-10], and – most conveniently – according to a "signal-on" or "signal-off" mechanism [11-13].

Recently, in order to improve the sensitivity of such electrochemical sensors, the use of gold, silver, platinum or silicate nanoparticles has been reported [14-22]. Colloidal nanoparticles have attracted attention because they can act both as transducers and as redox markers; examples include ultralow detection of DNA (AuNPs) [23-25] including single base mismatches (AgNPs) [26], the detection of avian influenza virus (AIV) H7 on graphene electrodes (AgNPs) [27], the determination of cholesterol on glassy carbon electrodes (AgNPs) [28], nanocomposite films of CuO Honeycombs/AgNPs for glucose detection [29], detecting tyrosine kinase-7 (methylene blue/AuNPs) [30], or porous-hollowed-silver-gold core-shell nanoparticles for prostate cancer detection [31]. Silver deposition onto gold nanoparticles gave signal enhancement in the range of two orders of magnitude [32]. Advantages of using NPs are in their ease of preparation, quantum characteristics, large surface area and excellent efficiency in electron transfer [33, 34]; furthermore, they can easily be modified with DNA, e.g. using avidin-biotin complexation [35] or *via* thiol-metal bond formation [36]. Table 1 gives an overview of the current detection limits that can be achieved with selected electrochemical sensors which contain nanoparticles for enhanced detection of oligonucleotides (ODNs).

Table 1. Comparison of the detection range and LOD of selected nanoparticle-based electrochemical genosensors.

Electrode modification	Analytical signal source	Linear Range [M]	Limit of detection [M]	Ref.
AuNP + ssDNA / ITOE	H	1×10^{-15} – 10×10^{-12}	1×10^{-15}	[20]
AuNP–ssDNA + MCH / PSS + PAH / MPA / AuE	$Ru(NH_3)_6^{3+}$	1.0×10^{-11} – 10×10^{-5}	1×10^{-11}	[21]
AuNP / TGA / MCH-hpDNA / AuE	$[Fe(CN)_6]^{3-/4}$	1.0×10^{-17} – 1.0×10^{-11}	1.7×10^{-18}	[22]
hpDNA / AuNP / rpDNA / tDNA / cpDNA / AuE	$[Ru(NH_3)_5L]^{2+}$	–	1×10^{-15}	[24]
AuNPs + ssDNA / Pt-UME	H	1×10^{-12} – 100×10^{-9}	1×10^{-12}	[25]
ssDNA–AuNPs / aDNA / AuNPs / Nf / GCE	MB	100×10^{-12} – 1×10^{-9}	372×10^{-15}	[30]
AuNP@Ag–tDNA / ssDNA / chitosan / GCE	Ag	1.0×10^{-10} – 5.0×10^{-9}	5×10^{-11}	[32]
AuNP–c-ssDNA) / SH-ssDNA + MCH / AuE	$[Co(phen)_3]^{3+/2+}$	0.51×10^{-12} – 8.58×10^{-12}	0.51×10^{-12}	[37]
ssDNA / Av / PAMAM / MPA / AuE	$Ru(NH_3)_6^{3+}$	1.4×10^{-11} – 2.7×10^{-14}	1.4×10^{-14}	[38]
(ss-DNA) / AgNP / PPAA / MWCNTs–COOH / GCE	adriamycin	9.0×10^{-12} – 9.0×10^{-9}	3.2×10^{-12}	[39]
ssDNA-S-AgNP / Pdop@Gr / GCE	MB	1.0×10^{-13} – 1.0×10^{-8}	3.2×10^{-15}	[40]
triplex-Ag/PtNCs / LNA / GCE	$[Fe(CN)_6]^{3-/4-}$	1.0×10^{-15} – 1×10^{-8}	0.8×10^{-15}	[41]
AuNP–P-ssDNA (1:200) / SH-ssDNA + MCH / AuE	CoP	5×10^{-17} – 1×10^{-16}	3.8×10^{-18}	[42]
AgNP–P-ssDNA (1:10) / SH-ssDNA + MCH / AuE	CoP	5×10^{-17} – 1×10^{-16}	5.0×10^{-18}	this work

Abbreviations: Pt UME: Platinum ultramicroelectrode, AuNPs: Gold nanoparticles, ssDNA: single stranded DNA, ITOE: Indium Tin oxide electrode, Nf: nafion, GCE: Glassy carbon electrode, hpDNA: Hairpin DNA, rpDNA: reporter DNA, tDNA: target DNA, cpDNA: capture DNA, aDNA: DNA aptamer, TGA: thioglycolic acid, MCH: 6-Mercapto-1-hexanol, AuE: Gold electrode, PAMAM: polyamidoamine, MPA: 3-mercaptopropionic acid, Av: avidin, MB: methylene blue, H: hydrazine, PSS: poly(styrene sulfonate), PAH: poly(allylamine hydrochloride), CoP: cobalt (II) porphyrin, Gr: graphene, AgNPs: silver nanoparticles, NCs: nanoclusters.

We have recently devised electrochemical genosensors that work on the basis of redox active cobalt porphyrins (CoP), which are attached to single stranded DNA probes and placed close to the gold electrode surface. The changes in the Co(II)/Co(III) Faradic current upon hybridisation with the complementary DNA can easily be measured, and a signal-off mechanism has been established [43]. The indications are that the CoP is placed in a more hydrophobic environment upon DNA hybridisation (major groove) and is thus not accessible to the electrolyte, giving a distinct drop in current. The limit of detection (LOD) was found to be in the femtomolar range and amounts to around 1000 DNA molecules in the analyte; the sensor showed excellent selectivity by detecting triple (non-adjacent) and single base-pair mismatches in the target sequence. By introducing 13 nm gold nanoparticles (AuNP) in-between the DNA probe and the gold electrode, the system could be improved to a LOD 3.8 attomolar and detecting as few as 23 DNA molecules [42]. The signal amplification was shown to arise from a higher loading of redox marker modified DNA on the gold electrode, and its performance is superior to most other electrochemical sensors (see Table 1). Scheme 1 shows the general procedure for the formation of the sensor system.

Whilst this is truly approaching single molecule detection using a simple analytical setup, we asked ourselves the questions whether changing the AuNP to the silver analogue (AgNP) would i) improve the detection limit, ii) influence the redox behaviour of the sensor and potentially leading to multiplexing on the same electrode, and iii) lead to a much cheaper manufacturing method compared to AuNP. Despite only very small quantities of the noble metal being used in the fabrication of the NP for one sensor, the price of $NaAuCl_4$ *vs* $AgNO_3$ differs by a factor of ~20, which has a significant impact in large-scale production. AgNPs have only rarely been used in the electrochemical detection of DNA, with significantly higher LODs than our system (Table 1); to our knowledge, AgNPs have not been attached to gold electrodes directly for the purpose of DNA detection but for general improvement of electron transfer at the interface of the gold electrode [44, 45]. The aim of this study was to specifically answer the questions set out above, which will help researchers to make a rational choice between AgNP or AuNP, based on their needs and resources.

Given that we have already produced a sensitive DNA sensor [42], we chose the same system but manufactured with AgNPs instead of AuNPs. We report the characterisation of the novel AgNP modified sensor and discuss the analogy and differences between the AuNP and AgNP systems in terms of electrochemical performance and DNA detection. For consistency with our previous work, we have chosen a sequence relevant to the detection of avian influenza virus H5N1, but the system would equally work with any other DNA sequence.

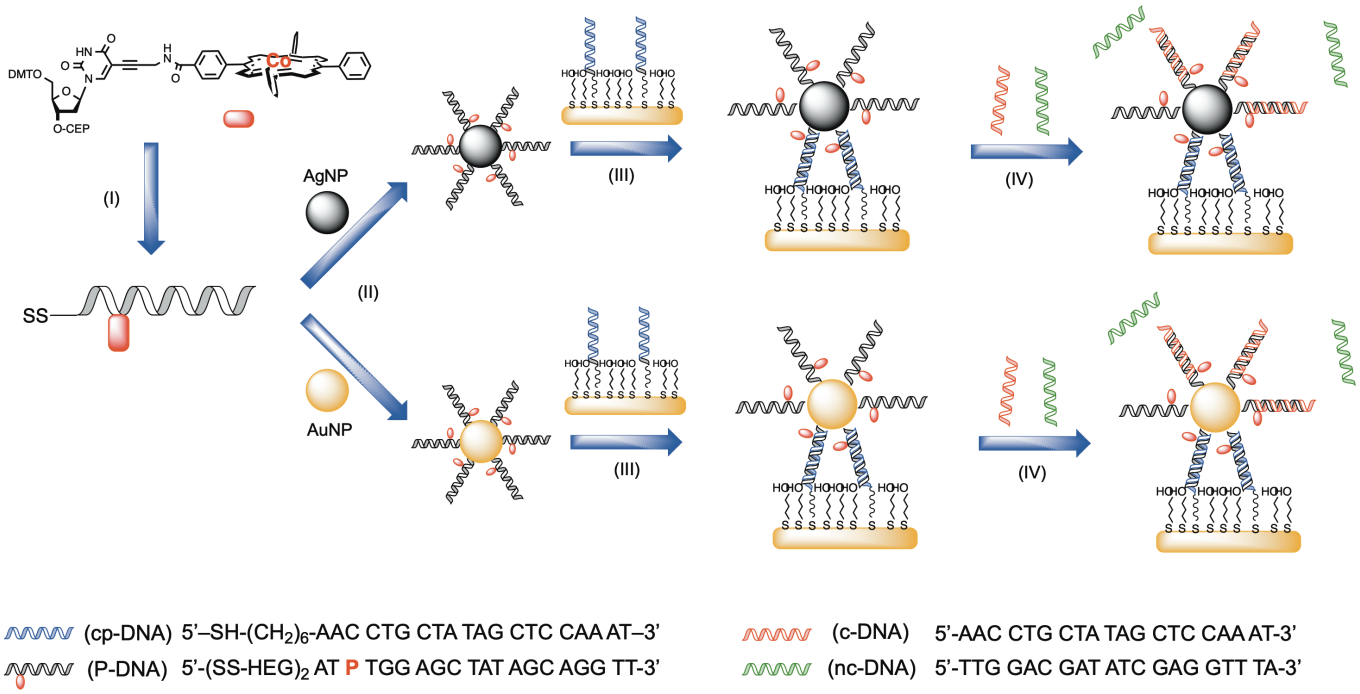

Scheme 1. Schematic representation of the general genosensor fabrication. (I) Synthesis of the DNA using standard phosphoramidite chemistry leads to the cobalt-porphyrin modified probe strand (P-DNA); DMT = dimethoxy trityl, CEP = β-cyano ethoxy phosphoramidite. (II) Attachment of the P-DNA to either AgNPs or AuNPs. (III) Partial hybridisation of the probe strands with the capture strands (cp-DNA, on gold surface within an MCH monolayer) to attach the NPs to the surface. (III) Hybridisation of the probe and complementary strands (c-DNA) for target detection; non-complementary DNA (nc-DNA) will not bind.

2. Experimental Section

2.1. Reagents and materials

6-Mercaptohexan-1-ol (MCH), Cyclohexane, buffer components: sodium chloride (NaCl), sodium phosphate monobasic (NaH_2PO_4) and sodium phosphate dibasic (Na_2HPO_4) were purchased from Sigma-Aldrich (Poznań, Poland). Potassium hydroxide (KOH), sulphuric acid (H_2SO_4), ethanol (EtOH) and methanol (MeOH) were obtained from Avantor Performance Materials (Gliwice, Poland). Trisodium citrate dihydrate, povidone (PVP), silver nitrate ($AgNO_3$), sodium borohydride ($NaBH_4$) were obtained from Sigma-Aldich (UK). Oligonucleotides apart from the cobalt-porphyrin (P-DNA), see below, were purchased from Biomers (Germany). The oligonucleotide tethered with a thiol linker abbreviated as cp-DNA (5'–SH-$(CH_2)_6$-AAC CTG CTA TAG CTC CAA AT–3') was

used as capturing probe for the immobilization of AgNP functionalised with DNA on the surface of gold electrodes via hybridisation. The oligonucleotide abbreviated as P-DNA (5'–$(SH\text{-}HEG)_2$-AT **P** TGG AGC TAT AGC AGG TT–3') was used as the detection probe, modified with CoP, and then immobilised on the surface of AgNP; this DNA was synthesized according to previously published methods [43]. Two unmodified oligonucleotides served as analytes, a complementary c-DNA (5'–AAC CTG CTA TAG CTC CAA AT–3') and a non-complementary nc-DNA (5'–TTG GAC GAT ATC GAG GTT TA–3'), respectively. All aqueous solutions were prepared with deionized and charcoal-treated water (resistivity of 18.2 $M\Omega \cdot cm^{-1}$) purified with a Milli-Q reagent grade water system (Millipore, Bedford, MA). All solutions were deoxygenated by purging with nitrogen (ultra-pure 6.0, Air Products, Poland) for 15 minutes. Each step of modification and hybridisation processes were performed in phosphate buffer (PB) containing 2.5 mM NaH_2PO_4, 2.5 mM Na_2HPO_4 and 50 mM NaCl, pH 7.0. The concentrations of the DNA dilutions were verified using UV absorption (NanoDrop).

2.2 Synthesis of silver nanoparticles functionalised with P-DNA

A trisodium citrate dihydrate solution (1.8 mL, 0.25 M) and PVP solution (1.8 mL, 0.25 M) were added to a solution of $AgNO_3$ (30 mL, 1.1 mM) and left stirring for 10 minutes. $NaBH_4$ solution (1.0 mL, 0.1 M) was added and the solution turned a dark yellow colour. This was repeated using a further 2 mL $NaBH_4$ solution to give a darker yellow solution. This solution was centrifuged for ten minutes and the clear supernatant removed. The AgNPs were re-dispersed in water and diluted to give a concentration of 0.2 µM.

P-DNA was attached to the AgNPs using the ratios of AgNP:P-DNA 1:10 and 1:200. AgNP solution (100 µL, 0.2 µM) was added to two vials, followed by P-DNA (100 µL) at 2 µM or 40 µM separately, to give two final concentrations of 1 µM and 20 µM for the DNA, and 0.1 µM for the AgNP. NaCl solution (200 µL, 0.125 M) and sodium phosphate buffer (100 µL, 25 mM, pH 7.0) were added to the AgNP–P-DNA solutions so that the total volume of each was increased to 500 µL. The solutions were then left for two hours, then their volume was slowly reduced to ~100 µL by vacuum centrifugation, to gradually increase the ionic strength and concentration of DNA.

The samples were then purified by centrifugation (13000 rpm, 15 minutes) and the supernatant removed. This purification step was repeated, and the solutions then stored at 4°C in a solution of 6 mM phosphate buffer containing 0.2 M NaCl, at a concentration of 0.1 µM AgNP.

The AgNP showed a range in size of the NPs from 5 – 25 nm according to TEM (see supporting information, Fig. S1) with smaller sizes dominating. Therefore, the reported value of $\varepsilon = 5.56 \times 10^{-8}$

(λ_{max} = 392 nm) was used for an average size of 11 nm AgNP, which also corresponds to the λ_{max} of 395 nm measured here, to calculate the concentration of the AgNP [46].

2.3 Preparation of genosensor: successive steps of the gold electrode modification

Gold disk electrodes with a radius of 1 mm (Bioanalytical Systems (BASi), West Lafayette, IN) were used for all experiments. The electrode preparation was performed according to already published protocol [42]**.** Briefly, the electrodes were polished with 0.3 μm and 0.05 μm alumina slurry (Buehler, Lake Bluff, IL USA) on a flat pads (BAS) for 5 min each and rinsed with Milli-Q water. They were further cleaned electrochemically by cyclic voltammetry (CV). At first, the electrodes were dipped in 0.5 M KOH solution and the potential was cycled between -0.4 V and -1.2 V (versus Ag/AgCl reference electrode) with a scan rate of 0.1 V/s and the number of cycles 6, 100 and 20. Subsequently, electrodes were cleaned in 0.5 M H_2SO_4 solution in the potential window between -0.3 V and +1.5 V (versus Ag/AgCl reference electrode) with a scan rate of 0.1 V/s and number of cycles 6, 20 and 6. After cleaning, the surfaces of gold electrodes were refreshed in 0.5 M KOH solution for 20 cycles. Before modification they were rinsed with Milli-Q water followed by PB solution (pH 7.0). Afterwards 10 μL of the following solution was dropped on each gold electrode surface: 0.1 μM cp-DNA and 10 μM MCH in PB for 3h at room temperature (RT). Then the electrodes were rinsed with the same buffer. In the second step of modification, 10 μL of 6 pM AgNP–P-DNA (1:10 or 1:200) dissolved in PB solution were dropped on the gold electrodes surfaces for 2h at RT. Finally, they were washed with the PB solution and stored in this buffer overnight at RT.

2.4 Electrochemical measurements

All electrochemical measurements were performed with a potentiostat-galvanostat AutoLab (Eco Chemie, Utrecht, The Netherlands) with a three-electrode configuration. Potentials were measured *vs.* the Ag/AgCl electrode, and a platinum wire was used as an auxiliary electrode. CV measurements were performed in the potential range from -0.100 V to +0.750 V for the modified gold electrodes. square wave voltammetry (SWV) was performed with a potential from -0.100 V to +0.750 V for the modified gold electrodes with a step potential of 0.001 V, a square-wave frequency of 50 Hz, and an amplitude of 0.050 V. Differential pulse voltammetry (DPV) was performed with a potential scanned in the potential window: -0.100 V to +0.750 V (oxidation) or +0.750 V to -0.100 V (reduction), with a step potential of 0.001 V, and an amplitude of 0.025 V. All measurements were carried out in the

presence of PB purged with nitrogen for 15 min. A gentle nitrogen flow was used over the sample solution during all measurements.

2.5 Hybridisation processes of the AgNP–P-DNA probe and the target sequences

The target oligonucleotides (c-DNA and nc-DNA) were diluted with the PB solution to the concentrations of 0.05, 0.075, 0.1 and 0.2 fM. Hybridisation reactions were performed by dropping 10 μL of the PB solution containing analytes c-DNA or nc-DNA on the modified gold electrode surface for 1 h at RT. After hybridisation with the particular concentration of targets, the electrodes were rinsed thoroughly with PB solution and placed into the cell for electrochemical measurements. The hybridisation processes were monitored using SWV. The electrode responses were expressed as: $(I_n–I_0)/I_0 \times 100\%$, where I_n is the peak current measured in the presence of the analyte and I_0 the peak current before applying the analyte i.e. in pure buffer.

In addition, before starting each experiment the stability of the genosensor was checked by dropping pure PB buffer solution and equilibrating for 1 h on the modified gold electrode surfaces and after that the current responses were measured by means of SWV before starting each experiment. The results confirmed the stability of all tested systems.

2.6 Atomic Force Microscopy measurements

Gold substrates modified with Au/SH-DNA+MCH/AgNP–P-DNA (1:10) were characterised by atomic force microscope (AFM) system from Universal SPM Quesant (Agoura Hills, CA, USA). As gold substrates mica plates coated with 10 nm thick titanium under layer and 100 nm thick gold (Imec, Belgium) were used. Before experiments, the gold substrates were rinsed with cyclohexane and cleaned using a UV/ozone chamber (Novascan Technologies, USA) for 20 min. Next, they were annealed by hydrogen flame. Modification layers were formed by immersion of the Au substrate in PB solution containing a mixture of 0.1 μM SH-DNA and 10 μM MCH (3h, RT). Then the substrate was rinsed with PB and dipped in the same buffer but containing 6 pM AgNP–P-DNA (1:10) for 2h at RT. Finally, it was washed with PB and stored in this buffer overnight at RT. The modification on gold plates proceeded analogously to that on the gold electrodes.

The AFM images were obtained using non-contact mode with NPC16 tip (W2C, Si_3N_4), which oscillates at *ca.* 170 kHz resonance frequency above the sample surface. The nominal spring constant of these cantilevers was equal to 45 N/m. The radius of tip curvature was *ca.* 10 nm. Images were recorded in air with pixel resolution of 300 × 300.

3. Results

3.1 Genosensor fabrication

The steps for the genosensor fabrication are shown in Scheme 1. In the first step (I), the gold electrode surface is modified with a thiol modified DNA capture probe (cp-DNA) embedded in 6-mercaptohexan-1-ol (MCH) self-assembled monolayer (SAM). The cp-DNA is complementary to the P-DNA. In the second step (II), AgNPs functionalised with P-DNA are immobilised on the gold electrode by hybridisation with the cp-DNA. As a consequence, some of P-DNA strands are used for binding of AgNP to the electrode surface, but most of them are not involved in this hybridisation and remain able to interact with target strands in the sample solution. During the last step (III), hybridisation between the P-DNA and target DNA (c-DNA) is carried out for signal generation. The non-complementary strand (nc-DNA) serves as negative control. To compare the influence of surface coverage of the AgNP with the probe – and of redox centres CoP – on the sensitivity of the sensor, we employed two different sensors, where a ratio of AgNP:P-DNA of 1:10 or 1:200 was used during the synthesis. This method to produce sensors with nanoparticle modification works very well for both gold and silver NPs and should be applicable to other types of nanoparticles or quantum dots, thus making it a very general approach.

3.2 AFM characterization of SH-DNA+MCH/AgNPs–P-DNA (1:10) layer

To visualise the topology of the gold surfaces after modification with the AgNP–P-DNA (1:10), non-contact mode of AFM in air was used. The topography of the AgNP–P-DNA layer deposited on the Au substrate (Fig. 1A) showed well-formed objects over the entire scanned range. The surface displays an RMS roughness equal to 67.9 ± 5.1 nm over 5×5 μm^2. The size of the objects was found to be 172.5 ± 9.2 nm. It should be noted that this is significantly larger than what would be expected from the AgNP coated with a single layer of DNA. The AgNP themselves show some fluctuation in size, ranging from 5 nm to 25 nm (Fig. S1); adding a 20-mer DNA would account for an additional 5 to 6 nm, thus an estimated radius range of 15 to 37 nm could be expected.

Compared to the AuNP surface (Fig. 1B), there are clear differences. Firstly, the AgNP surface shows a much larger RMS roughness compared to the AuNP surface, which showed a roughness of 48.7 ± 7.4 nm. Secondly, while the AuNP surface shows better separated NPs with little to no aggregation, the AgNP surface reveals a high level of coverage with AgNP. The average size of the AuNP was 85.7 ± 4.2 nm where the increase in size can be explained by the attachment of DNA [42]; in the AgNP surface, however, the increase in particle size

far exceeds the size of the DNA. Therefore, it can be assumed that a significant amount of clustering is present in the AgNP system.

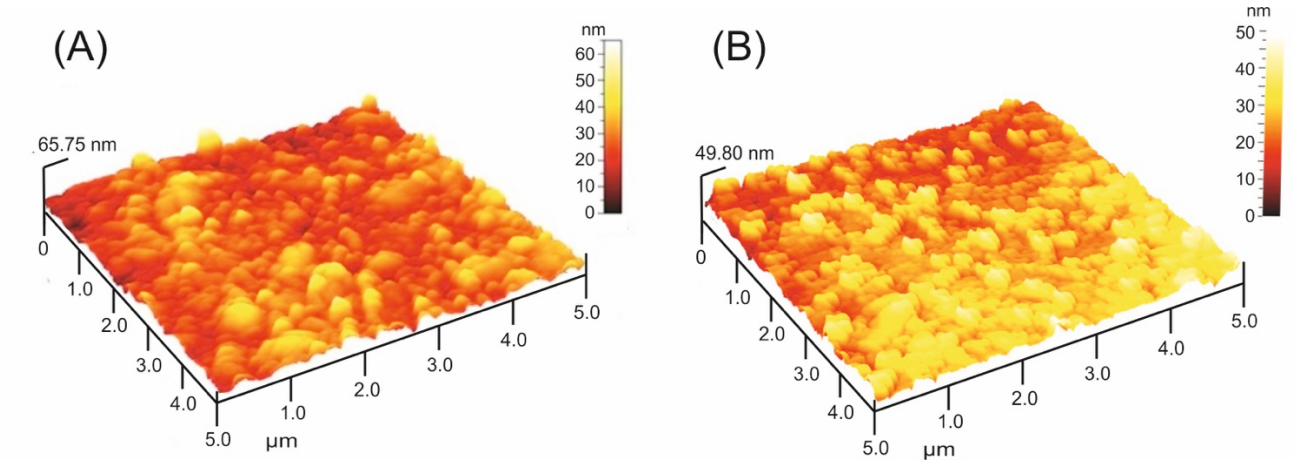

Fig. 1. AFM images gold Au(111) thin film on mica substrate modified with (A) AgNP–P-DNA (1:10), and (B) with AuNP–P-DNA (1:200).

3.3 Electrochemical characterisation of the redox-active layers consisting of AgNPs-P-DNA with different ratios (1:10 and 1: 200)

To fully characterise the electrochemical properties of the sensors with either AgNP–P-DNA = 1:10 or 1:200, they were analysed using CV, SWV and DPV. Both sensors exhibited well-defined quasi-reversible Co(II)/Co(III) redox peaks (Fig. S2, S3). Slightly higher current intensities were obtained for the system incorporated AgNP–P-DNA at a ratio of 1:10, and the peak potentials for this system were fractionally shifted towards positive values in comparison to that which incorporated the AgNP–P-DNA (1:200) system. The electrochemical parameters (peak positions and current values) obtained are summarised in Table S1 and reveal that they are essentially the same as previously measured with the AuNP-system [42]. Therefore, the change from gold to silver does not affect the redox behaviour of the cobalt porphyrin, confirming that the electron transfer reaction does not involve the nanoparticle.

Confirmation that the redox centres are located on the electrode surface was obtained from measuring the peak currents at different scan rates. Both AgNP sensors become more irreversible with increasing scan rates and exhibit a linear relationship between scan rate and peak current (anodic or cathodic), showing that the redox process is not diffusion controlled [47, 48] (see ESI). From these data, the density of redox active layers *(Γ)*, the electron transfer

coefficient *(α)* and the electrode reaction standard rate constant (k_s) were calculated (Table 2) [49]. For the AgNP–P-DNA (1:10) sensor, the data show lower Γ, higher α and lower k_s values than for the AgNP–P-DNA (1:200) sensor, as expected. The redox centre density increases with increasing DNA loading on the AgNP, and the values of $8.51 \pm 0.21 \times 10^{-12}$ (1:10) and $1.03 \pm 0.142 \times 10^{-11}$ (1:200) mol/cm^2 are slightly lower than the AuNP system ($\Gamma \cong 2.9 \times 10^{-11}$ mol/cm^2). The α-values of 0.62 and 0.81 are in the same range as for the AuNP modified electrodes ($\alpha = 0.66 - 0.74$), but the k_s-values ($0.8 - 0.9$ s^{-1}) are slightly higher than in the AuNP electrodes ($k_s = 0.7$ s^{-1}), thus the AgNP seems to induce a slightly faster redox reaction. Whether this is due to the slightly smaller size of the AgNPs is difficult to assess but could provide an explanation.

Table 2. Electrochemical parameters and limit of detection (LOD) of the modified gold electrodes (n=4) with either AuNPs or AgNPs.

Modifier	Γ / mol/cm^2 [a]	α [b]	k_s / s^{-1} [c]	LOD / M^{-1}
AgNP–P-DNA (1:10)	$8.51 \pm 0.21 \times 10^{-12}$	0.81 ± 0.02	0.81 ± 0.06	5.03×10^{-18}
AuNP–P-DNA (1:10) [d]	$3.0 \pm 0.2 \times 10^{-11}$	0.74 ± 0.15	0.70 ± 0.13	4.8×10^{-17}
AgNP–P-DNA (1:200)	$1.03 \pm 0.142 \times 10^{-11}$	0.62 ± 0.03	0.91 ± 0.02	8.72×10^{-18}
AuNP–P-DNA (1:200) [d]	$2.9 \pm 0.5 \times 10^{-11}$	0.68 ± 0.04	0.71 ± 0.02	3.8×10^{-18}

[a] Density of redox active layer; [b] electron transfer coefficient; [c] electrode reaction standard rate constant; [d] data taken from ref [42].

3.4 Detection of 20-mer DNA sequences

The detection of complementary c-DNA was done in the range of 0.05 – 0.20 fM after incubation for one hour and using SWV (Fig. 2A, B). Hybridisation with the target c-DNA caused a decrease in the Co(II)/Co(III) Faradic current for both biosensors, analogous as was observed for the AuNP-system [42]. The nc-DNA induced only small changes in the current, showing good selectivity for the complementary DNA (Fig. S4). For both AgNP sensors, a linear range for the concentration dependent response to c-DNA was observed from 50×10^{18} to 100×10^{-18} M (Fig. 2C), where a lower loading (1:10) seems to be beneficiary to obtain more sensitive genosensors as the response was more reproducible. The limit of detection (LOD) was calculated according to $LOD = 3.3\ \sigma/S$, where σ is the standard deviation of the response and S is the slope of the calibration curve [50]. The LODs for AgNP–P-DNA (1:10) and AgNP–P-DNA (1:200) were found to be 5.03×10^{-18} M and 8.72×10^{-18} M, respectively,

which are only slightly higher than for the AuNP sensors (Table 2). For the incubation we used 10 µL of the DNA target. Thus, taking into account sample volume and LOD, we can conclude that we are able to detect a minimum of 30 and 52 DNA molecules, using AgNP–P-DNA (1:10) or AgNP–P-DNA (1:200) system, respectively. This again compares well to the AuNP system with detection numbers of 290 (1:10) and 23 (1:200) molecules [42].

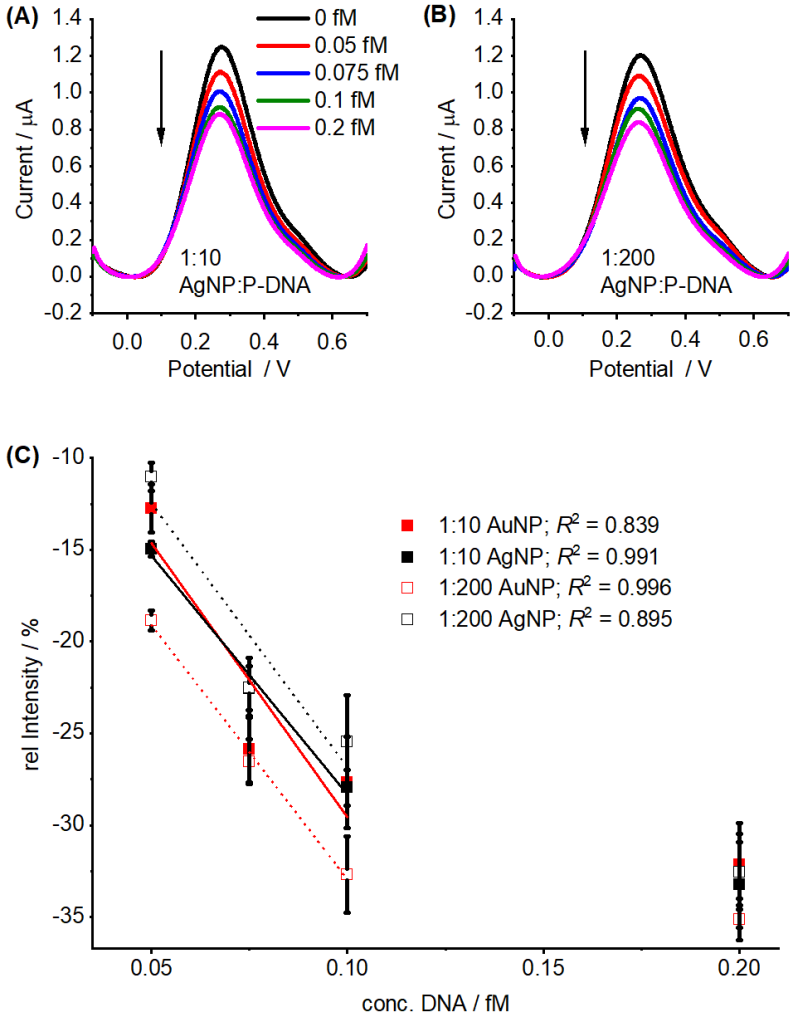

Fig. 2. Representative square-wave voltammograms recorded in PB buffer using gold electrodes modified with (A) AgNP–P-DNA (1:10); (B) AgNP–P-DNA (1:200). The responses were recorded before (black lines) and after hybridisation in PB buffer with complementary c-DNA. (C) Comparison of the relative intensity of $I=[(I_n-I_0)/I_0]\times100\%$ for the redox couple Co(II)/Co(III) current *vs.* concentration of AgNP (black) and AuNP (red [42]) modified electrodes; (■) NP–P-DNA (1:10), (□) NP–P-DNA (1:200).

The term "response ratio" was recommended for the selectivity determination of amperometric sensors, which is calculated from the ratio of the slopes of the calibration curves (sensitivities) of target and interfering compounds (nc-DNA) as the measure of selectivity ($R_{i,j}=S_j/S_i$) [31,32]. The parameters for our sensors are given in Table 3, together with the values calculated for the previous DNA sensors based on AuNPs [42]. The slopes of the calibration curves for c-DNA for the sensing system based on AgNP as well as AuNP are very

similar with a drop in relative intensity of ~15 % in all cases, confirming the comparable detection limits in the attomolar range (Fig. 2C). The slopes concerning nc-DNA were substantially lower, and the sensing systems show values of $R_{ij} < 1.0$, indicating very good selectivity. The lack of selectivity was only observed in the case of electrodes which incorporated AuNP-P-DNA (1:10) [42]. Also, the sensors based on AgNP-P-DNA (1:10) and AuNP-P-DNA (1:200) showed a better linear response (Fig. 2C).

Table 3. Selectivity comparing AgNP and AuNP modified sensors.

Sensor	**c-DNA**	**nc-DNA**	
	Slope S_i [%/fM]	**Slope S_j [%/fM]**	**Response ratio $R_{ij}=S_j/S_i$**
AgNP–P-DNA (1:10)	-260.00	-115.20	0.44
AgNP–P-DNA (1:200)	-287.80	-144.59	0.50
AuNP–P-DNA (1:10)[a)]	-298.60	-338.60	1.13
AuNP–P-DNA (1:200)[a)]	-276.80	-116.00	0.42

[a)] data taken from ref [42].

4. Discussion

Here we have prepared a DNA sensor which contains silver nanoparticles as a means to improve the sensitivity compared to unmodified gold electrodes. The system is analogous to our previously described sensor containing gold nanoparticles. The fabrication of both AuNP and AgNP sensors follows a general scheme, which demonstrates the versatility of the approach. The AgNP system proved to be slightly trickier to manufacture due to the instability of the AgNPs when exposed to light, but with careful handling this can easily be overcome. A direct comparison of the AgNP and AuNP systems allows for the first time to get an insight into sensors where the NPs are attached to the electrode surface as close as possible, but not in direct contact, and where the NPs are not part of a hybridisation process with either probe or target DNA strand.

We have set out to answer some basic questions regarding sensitivity, multiplexing and economics comparing both AgNP and AuNP modified sensors. With regards to performance, is there any benefit for using either gold or silver? The short answer is No. Both types of sensors show a response that it dominated by the cobalt-porphyrin redox marker, and the electron transfer does not involve either type of NP. They all show a linear response in the attomolar concentration range of

target DNA, very good selectivity towards complementary DNA *vs* non-complementary DNA, and detection limits that are approaching single molecule detection. This leads to the second question: can a mixture of AgNPs and AuNPs on the same electrode lead to the detection of different DNA sequences on the same electrode? The answer again is No, at least not with our system. In this respect, gold and silver are equal; whether this holds true for other nanoparticles and quantum dots, other attachment technologies, or ratiometric detection [51] remains to be seen.

Differences in the two systems arise from the coverage of the electrode surface. In case of gold NPs, the particles are better separated, and no aggregation is observed. This is not only the case for the saturated NPs in terms of DNA loading, which we determined to be around 160 DNA molecules per NP [42], but for lower loadings as well. The silver NP system, on the other hand, shows a substantial amount of aggregation on the surface, irrespective of DNA loading on the NP. Since the detection of the redox signal arises from the cobalt-porphyrin and does not seem to involve the NPs, we conclude that the aggregation itself does not impact the performance of the sensor. The best performing systems contain either AuNPs with a high loading of DNA, or AgNPs with a low loading of DNA. It is not quite clear why the lower loading of DNA on the AgNPs is beneficiary. From an economic point-of-view, this means that the AgNP modified electrode benefits from the use of a much lower loading of DNA probe on the nanoparticles which is compensated by a higher coverage of the electrode with the NP, which results in a much better DNA economy, and from cheaper starting materials (Ag *vs.* Au), thus leads to more affordable yet highly sensitive sensors.

Taking reproducibility, selectivity and LOD into account, in the case of AgNPs the loading of 1:10 gives the best results, whereas in the case of AuNP the loading of 1:200 gives the most successful electrode. Our recommendation therefore is to use AgNPs if an easy-to-setup system for testing in the laboratory is required, but to consider AgNPs is upscaling is the aim.

5. Acknowledgments

This research was performed with statutory funds of Biosensors Department Institute of Animal Reproduction and Food Research, Polish Academy of Sciences, and from the University of Southampton, UK. Funding from the European Union for IM in form of a Marie Skłodowska-Curie Fellowship ‘‘Nano-DNA’’ (FP7-PEOPLE-2012-IEF, No. 331952), from the BBSRC [BB/M025624/1], and from the National Science Centre, Poland [grant no. 2016/21/B/ST4/03834] is greatly acknowledged.

6. Conflicts of interest

There are no conflicts to declare.

7. References

[1] A. Gattani, S. V. Singh, A. Agrawal, M. H. Khan , P. Singh, Recent progress in electrochemical biosensors as point of care diagnostics in livestock health, Anal. Biochem. 579 (2019) 25-34. https://doi.org/10.1016/j.ab.2019.05.014

[2] Y. J. Chen, C. Qian, C. Z. Liu, H. Shen, Z. J. Wang, J. F. Ping, J. Wu , H. Chen, Nucleic acid amplification free biosensors for pathogen detection, Biosens. Bioelectron. 153 (2020) 17. https://doi.org/10.1016/j.bios.2020.112049

[3] S. Campuzano, P. Yanez-Sedeno , J. M. Pingarron, Molecular Biosensors for Electrochemical Detection of Infectious Pathogens in Liquid Biopsies: Current Trends and Challenges, Sensors 17 (2017) 21. https://doi.org/10.3390/s17112533

[4] C. E. Jin, T. Y. Lee, B. Koo, H. Sung, S. H. Kim , Y. Shin, Rapid virus diagnostic system using bio-optical sensor and microfluidic sample processing, Sens. Actuator B-Chem. 255 (2018) 2399-2406. https://doi.org/10.1016/j.snb.2017.08.197

[5] P. R. Miller, R. J. Narayan , R. Polsky, Microneedle-based sensors for medical diagnosis, J. Mat. Chem. B 4 (2016) 1379-1383. https://doi.org/10.1039/c5tb02421h

[6] E. Palecek , M. Bartosik, Electrochemistry of Nucleic Acids, Chem. Rev. 112 (2012) 3427-3481. https://doi.org/10.1021/cr200303p

[7] H. Aoki , Y. Umezawa, High Sensitive Ion-Channel Sensors for Detection of Oligonucleotides Using PNA Modified Gold Electrodes, Electroanalysis 14 (2002) 1405-1410. https://doi.org/10.1002/1521-4109(200211)14:19/20<1405::AID-ELAN1405>3.0.CO;2-G

[8] H. Aoki , Y. Umezawa, Trace analysis of an oligonucleotide with a specific sequence using PNA-based ion-channel sensors, Analyst 128 (2003) 681-685. https://doi.org/10.1039/b300465a

[9] K. Kurzątkowska, A. Sirko, W. Zagórski-Ostoja, W. Dehaen, H. Radecka , J. Radecki, Electrochemical Label-free and Reagentless Genosensor Based on an Ion Barrier Switch-off System for DNA Sequence-Specific Detection of the Avian Influenza Virus, Anal. Chem. 87 (2015) 9702-9709.

[10] K. Malecka, A. Stachyra, A. Góra-Sochacka, A. Sirko, W. Zagórski-Ostoja, W. Dehaen, H. Radecka , J. Radecki, New redox-active layer create via epoxy–amine reaction – The base of genosensor for the detection of specific DNA and RNA sequences of avian influenza virus H5N1, Biosens. Bioelectron. 65 (2015) 427-434. https://doi.org/https://doi.org/10.1016/j.bios.2014.10.069

[11] C. H. Fan, K. W. Plaxco , A. J. Heeger, Electrochemical interrogation of conformational changes as a reagentless method for the sequence-specific detection of DNA, Proc. Natl. Acad. Sci. U. S. A. 100 (2003) 9134-9137. https://doi.org/10.1073/pnas.1633515100
[12] Y. Xiao, A. A. Lubin, B. R. Baker, K. W. Plaxco , A. J. Heeger, Single-step electronic detection of femtomolar DNA by target-induced strand displacement in an electrode-bound duplex, Proc. Natl. Acad. Sci. U. S. A. 103 (2006) 16677-16680. https://doi.org/10.1073/pnas.0607693103
[13] I. Grabowska, K. Malecka, A. Stachyra, A. Góra-Sochacka, A. Sirko, W. Zagórski-Ostoja, H. Radecka , J. Radecki, Single Electrode Genosensor for Simultaneous Determination of Sequences Encoding Hemagglutinin and Neuraminidase of Avian Influenza Virus Type H5N1, Anal. Chem. 85 (2013) 10167-10173. https://doi.org/10.1021/ac401547h
[14] E. Bagheri, L. Ansari, E. Sameiyan, K. Abnous, S. M. Taghdisi, M. Ramezani , M. Alibolandi, Sensors design based on hybrid gold-silica nanostructures, Biosens. Bioelectron. 153 (2020) 112054. https://doi.org/10.1016/j.bios.2020.112054
[15] H. K. Kordasht, M. Pazhuhi, P. Pashazadeh-Panahi, M. Hasanzadeh , N. Shadjou, Multifunctional aptasensors based on mesoporous silica nanoparticles as an efficient platform for bioanalytical applications: Recent advances, Trac-Trends Anal. Chem. 124 (2020) 15. https://doi.org/10.1016/j.trac.2019.115778
[16] U. Jarocka, R. Sawicka, A. Gora-Sochacka, A. Sirko, W. Dehaen, J. Radecki , H. Radecka, An electrochemical immunosensor based on a 4,4 '-thiobisbenzenethiol self-assembled monolayer for the detection of hemagglutinin from avian influenza virus H5N1, Sens. Actuator B-Chem. 228 (2016) 25-30. https://doi.org/10.1016/j.snb.2016.01.001
[17] U. Jarocka, R. Sawicka, A. Gora-Sochacka, A. Sirko, W. Zagorski-Ostoja, J. Radecki , H. Radecka, An Immunosensor Based on Antibody Binding Fragments Attached to Gold Nanoparticles for the Detection of Peptides Derived from Avian Influenza Hemagglutinin H5, Sensors 14 (2014) 15714-15728. https://doi.org/10.3390/s140915714
[18] S. J. Kwon , A. J. Bard, DNA Analysis by Application of Pt Nanoparticle Electrochemical Amplification with Single Label Response, J. Am. Chem. Soc. 134 (2012) 10777-10779. https://doi.org/10.1021/ja304074f
[19] Kashish, S. Gupta, S. K. Dubey , R. Prakash, Genosensor based on a nanostructured, platinum-modified glassy carbon electrode for Listeria detection, Anal. Methods, 7 (2015) 2616-2622. https://doi.org/10.1039/C5AY00167F

[20] J. Das , H. Yang, Enhancement of Electrocatalytic Activity of DNA-Conjugated Gold Nanoparticles and Its Application to DNA Detection, J. Phys. Chem. C 113 (2009) 6093-6099. https://doi.org/10.1021/jp809850f
[21] S. F. Liu, J. Liu, L. Wang , F. Zhao, Development of electrochemical DNA biosensor based on gold nanoparticle modified electrode by electroless deposition, Bioelectrochemistry 79 (2010) 37-42. https://doi.org/10.1016/j.bioelechem.2009.10.005
[22] S. L. Li, W. W. Qiu, X. Zhang, J. C. Ni, F. Gao , Q. X. Wang, A high-performance DNA biosensor based on the assembly of gold nanoparticles on the terminal of hairpin-structured probe DNA, Sens. Actuator B-Chem. 223 (2016) 861-867. https://doi.org/10.1016/j.snb.2015.09.121
[23] L. Esfandiari, M. Lorenzini, G. Kocharyan, H. G. Monbouquette , J. J. Schmidt, Sequence-Specific DNA Detection at 10 fM by Electromechanical Signal Transduction, Anal. Chem. 86 (2014) 9638-9643. https://doi.org/10.1021/ac5021408
[24] H. F. Cui, T. B. Xu, Y. L. Sun, A. W. Zhou, Y. H. Cui, W. Liu , J. H. T. Luong, Hairpin DNA as a Biobarcode Modified on Gold Nanoparticles for Electrochemical DNA Detection, Anal. Chem. 87 (2015) 1358-1365. https://doi.org/10.1021/ac504206n
[25] J. Liu, M. Tian , Z. Liang, DNA analysis based on the electrocatalytic amplification of gold nanoparticles, Electrochim. Acta 113 (2013) 186-193. https://doi.org/10.1016/j.electacta.2013.09.111
[26] M. A. Mehrgardi , L. E. Ahangar, Silver nanoparticles as redox reporters for the amplified electrochemical detection of the single base mismatches, Biosens. Bioelectron. 26 (2011) 4308-4313. https://doi.org/https://doi.org/10.1016/j.bios.2011.04.020
[27] J. L. Huang, Z. X. Xie, Z. Q. Xie, S. S. Luo, L. J. Xie, L. Huang, Q. Fan, Y. F. Zhang, S. Wang , T. T. Zeng, Silver nanoparticles coated graphene electrochemical sensor for the ultrasensitive analysis of avian influenza virus H7, Anal. Chim. Acta 913 (2016) 121-127. https://doi.org/10.1016/j.aca.2016.01.050
[28] S. Nantaphol, O. Chailapakul , W. Siangproh, Sensitive and selective electrochemical sensor using silver nanoparticles modified glassy carbon electrode for determination of cholesterol in bovine serum, Sens. Actuator B-Chem. 207 (2015) 193-198. https://doi.org/10.1016/j.snb.2014.10.041
[29] M. Baghayeri, M. Nodehi, A. Amiri, N. Amirzadeh, R. Behazin , M. Z. Iqbal, Electrode designed with a nanocomposite film of CuO Honeycombs/Ag nanoparticles electrogenerated on a magnetic platform as an amperometric glucose sensor, Anal. Chim. Acta 1111 (2020) 49-59. https://doi.org/10.1016/j.aca.2020.03.039

[30] X. Miao, Z. Li, A. Zhu, Z. Feng, J. Tian , X. Peng, Ultrasensitive electrochemical detection of protein tyrosine kinase-7 by gold nanoparticles and methylene blue assisted signal amplification, Biosens. Bioelectron. 83 (2016) 39-44. https://doi.org/https://doi.org/10.1016/j.bios.2016.04.032
[31] C. Pothipor, N. Wiriyakun, T. Putnin, A. Ngamaroonchote, J. Jakmunee, K. Ounnunkad, R. Laocharoensuk , N. Aroonyadet, Highly sensitive biosensor based on graphene-poly (3-aminobenzoic acid) modified electrodes and porous-hollowed-silver-gold nanoparticle labelling for prostate cancer detection, Sens. Actuator B-Chem. 296 (2019) 9. https://doi.org/10.1016/j.snb.2019.126657
[32] H. Cai, Y. Q. Wang, P. G. He , Y. H. Fang, Electrochemical detection of DNA hybridization based on silver-enhanced gold nanoparticle label, Anal Chim Acta 469 (2002) 165-172. https://doi.org/10.1016/S0003-2670(02)00670-0
[33] S. Y. Liu, X. D. Tian, Y. Zhang , J. F. Li, Quantitative Surface-Enhanced Raman Spectroscopy through the Interface-Assisted Self-Assembly of Three-Dimensional Silver Nanorod Substrates, Anal. Chem. 90 (2018) 7275-7282. https://doi.org/10.1021/acs.analchem.8b00488
[34] J. W. Zheng, G. Chumanov , T. M. Cotton, Photoinduced electron transfer at the surface of nanosized silver particles as monitored by EPR spectroscopy, Chem. Phys. Lett. 349 (2001) 367-370. https://doi.org/10.1016/s0009-2614(01)01149-6
[35] C. Kokkinos, Electrochemical DNA Biosensors Based on Labeling with Nanoparticles, Nanomaterials (Basel) 9 (2019) 1361. https://doi.org/10.3390/nano9101361
[36] A. Heuer-Jungemann, R. Kirkwood, A. H. El-Sagheer, T. Brown , A. G. Kanaras, Copper-free click chemistry as an emerging tool for the programmed ligation of DNA-functionalised gold nanoparticles, Nanoscale 5 (2013) 7209-12. https://doi.org/10.1039/c3nr02362a
[37] Z. L. Zhang, D. W. Pang, H. Yuan, R. X. Cai , H. Abruna, Electrochemical DNA sensing based on gold nanoparticle amplification, Anal. Bioanal. Chem. 381 (2005) 833-838. https://doi.org/10.1007/s00216-004-2972-8
[38] G. J. Li, X. L. Li, J. Wan , S. S. Zhang, Dendrimers-based DNA biosensors for highly sensitive electrochemical detection of DNA hybridization using reporter probe DNA modified with Au nanoparticles, Biosens. Bioelectron. 24 (2009) 3281-3287. https://doi.org/10.1016/j.bios.2009.04.022
[39] Y. Zhang, K. Zhang , H. Ma, Electrochemical DNA biosensor based on silver nanoparticles/poly(3-(3-pyridyl) acrylic acid)/carbon nanotubes modified electrode, Anal. Biochem. 387 (2009) 13-19. https://doi.org/10.1016/j.ab.2008.10.043

[40] K. J. Huang, Y. J. Liu, H. B. Wang , Y. Y. Wang, A sensitive electrochemical DNA biosensor based on silver nanoparticles-polydopamine@graphene composite, Electrochim Acta 118 (2014) 130-137. https://doi.org/10.1016/j.electacta.2013.12.019
[41] F. Wu, Q. Lin, L. Wang, Y. Zou, M. Chen, Y. Xia, J. Lan , J. Chen, A DNA electrochemical biosensor based on triplex DNA-templated Ag/Pt nanoclusters for the detection of single-nucleotide variant, Talanta 207 (2020) 120257. https://doi.org/10.1016/j.talanta.2019.120257
[42] B. Kaur, K. Malecka, D. A. Cristaldi, C. S. Chay, I. Mames, H. Radecka, J. Radecki , E. Stulz, Approaching single DNA molecule detection with an ultrasensitive electrochemical genosensor based on gold nanoparticles and cobalt-porphyrin DNA conjugates, Chem. Commun. 54 (2018) 11108-11111. https://doi.org/10.1039/c8cc05362f
[43] I. Grabowska, D. G. Singleton, A. Stachyra, A. Gora-Sochacka, A. Sirko, W. Zagorski-Ostoja, H. Radecka, E. Stulz , J. Radecki, A highly sensitive electrochemical genosensor based on Co-porphyrin-labelled DNA, Chem. Commun. 50 (2014) 4196-4199. https://doi.org/10.1039/c4cc00172a
[44] A. Arvinte, I. A. Crudu, F. Doroftei, D. Timpu , M. Pinteala, Electrochemical codeposition of silver-gold nanoparticles on CNT-based electrode and their performance in electrocatalysis of dopamine, J Electroanal Chem 829 (2018) 184-193. https://doi.org/10.1016/j.jelechem.2018.10.017
[45] P. Kar, F. Tatard, G. Lamblin, P. Banet, P. H. Aubert, C. Plesse , C. Chevrot, Silver nanoparticles to improve electron transfer at interfaces of gold electrodes modified by biotin or avidin, J Electroanal Chem 692 (2013) 17-25. https://doi.org/10.1016/j.jelechem.2012.12.020
[46] D. Paramelle, A. Sadovoy, S. Gorelik, P. Free, J. Hobley , D. G. Fernig, A rapid method to estimate the concentration of citrate capped silver nanoparticles from UV-visible light spectra, Analyst 139 (2014) 4855-4861. https://doi.org/10.1039/c4an00978a
[47] H. O. Finklea , D. D. Hanshew, Electron-transfer kinetics in organized thiol monolayers with attached pentaammine(pyridine)ruthenium redox centers, J. Am. Chem. Soc. 114 (1992) 3173-3181. https://doi.org/10.1021/ja00035a001
[48] A. J. Bard , L. R. Faulkner, Electrochemical Methods: Fundamentals and Applications, Wiley New York, 1980.
[49] E. Laviron, The use of linear potential sweep voltammetry and of ac voltammetry for the study of the surface electrochemical reaction of strongly adsorbed systems and of redox modified electrodes, J. Electroanal. Chem. Interfacial Electrochem. 100 (1979) 263-270.

[50] C. Macca , J. Wang, Experimental procedures for the determination of amperometric selectivity coefficients, Anal. Chim. Acta 303 (1995) 265-274. https://doi.org/10.1016/0003-2670(94)00511-j
[51] H. Jin, R. J. Gui, J. B. Yu, W. Lv , Z. H. Wang, Fabrication strategies, sensing modes and analytical applications of ratiometric electrochemical biosensors, Biosens. Bioelectron. 91 (2017) 523-537. https://doi.org/10.1016/j.bios.2017.01.011